



Variation of Vickers microhardness and compression strength of the bioceramics based on hydroxyapatite by adding the multi-walled carbon nanotubes

M. S. Barabashko^{1,2} · M. V. Tkachenko³ · A. A. Neiman⁴ · A. N. Ponomarev⁴ · A. E. Rezvanova⁵

Received: 12 December 2018 / Accepted: 19 March 2019 / Published online: 25 March 2019
© King Abdulaziz City for Science and Technology 2019

Abstract

Calcium phosphate ceramics for medical applications with additives of multi-walled carbon nanotubes were synthesized at a temperature of 1100 °C in the argon atmosphere. The concentration of nanotubes ranged from 0.05 to 0.5 wt.%. The morphology and structure of the powder of multi-walled carbon nanotubes and calcium phosphate ceramics have been characterized by the electron microscope. The most part of the initial nanotubes have distributions of outer diameter 10–25 nm. The multi-walled carbon nanotubes are located in the intergranular space, change their shape and aspect ratio. Diffraction patterns of ceramics show that all samples have apatite structure and any distinct reflections except those of hydroxyapatite are detected. The partial carbonization of ceramics is indicated by the results of FT-IR studies. With an increase of the amount of nanotubes in composite ceramics, the intensity of the carbonate stretching band increases, which may be due to partial oxidation of the nanotubes and as a result leads to more intensive carbonization of the apatite phase. It was found that the mechanical properties of ceramics (compression strength and Vickers microhardness) were improved with the increasing of the amount of nanotubes.

Keywords Hydroxyapatite · Multi-walled carbon nanotubes · Calcium phosphate ceramics · Mechanical properties · Compression strength · Vickers microhardness

Introduction

Calcium phosphate biomaterials are used in the medicine for filling the bone defects and voids, for bone reconstruction and coating the metal implants (Jadalannagari et al. 2013; Mansour et al. 2015; Puvvada et al. 2012; Buazar et al. 2014;

Kwok et al. 2009). Ceramics based on hydroxyapatite (HAp) have excellent biocompatibility, bioactivity, osteoconductivity, porosity and longer degradation time in comparison with other implant materials for orthopedic and dental medicine (Díaz et al. 2009).

One of the disadvantages of HAp is that the mechanical properties of this ceramic are weak. In this regard, the use of HAp in load-bearing orthopedic implants (pins, screws, plates, and spinal fusion bodies) is limited by its poor mechanical properties (Ahn et al. 2005). Its medical use is limited to making the low mechanical strength implants, powders and coatings.

It is important, to note, that the increase of the mineral content in the bones with the change of the human age leads to the decreasing of the water content and as a result can change the hardness in 1.5–2 times (Table 2 in Faingold et al. 2014).

Creations of new ceramic materials based on HAp with functional (including mechanical) characteristics close to those of natural bone can impact the creation of new technologies that provide the increasing of the role of personalized

✉ M. S. Barabashko
msbarabashko@gmail.com

¹ B. Verkin Institute for Low Temperature Physics and Engineering of NAS of Ukraine, 47 Nauky Ave., Kharkiv 61103, Ukraine

² National Research Tomsk Polytechnic University, 30 Lenin Ave., Tomsk 634050, Russia

³ V.N. Karazin Kharkiv National University, 4, Maidan Svobody, Kharkiv 61077, Ukraine

⁴ Institute of Strength Physics and Materials Science of SB RAS, 2/4 Akademicheskoy Ave., Tomsk 634055, Russia

⁵ Tomsk State University of Control Systems and Radioelectronics, 40 Lenin Ave., Tomsk 634050, Russia

medicine, high-tech healthcare and health preservation technologies in human life. To increase the strength and hardness of the implants, reinforcing agents are added to the HAp ceramics. Such reinforcing agents are zirconia (Sung et al. 2007; Padovani et al. 2015), alumina (Shrivastava et al. 2009; Radha et al. 2015), HAp whiskers (Zhang et al. 2014; Yang et al. 2014), silver (Mocanu et al. 2014; Ai et al. 2017), titanium and titanium alloys (Goudarzi et al. 2014; Zhang et al. 2010) and others (Phan et al. 2016; Kumar et al. 2015; Supraja et al. 2015; Ol'khovik et al. 2011).

There are some difficulties that should be solved to get these advantages: reinforcing agents should not reduce the biocompatibility and bioactivity of the implants; most of the materials reduce the ability to form a stable interface between the composite and the bone; in HAp ceramics it is necessary to add the large amounts of reinforcing phases; metals and zirconium can be degraded and have corrosion; some mechanical stresses can lead to the destruction of bone tissue near the implant, if the Young modulus and the hardness of a metal implant, for example, titanium, is significantly greater than that of a bone. Long fibers, such as Al_2O_3 , ZrO_2 , SiC , and Si_3N_4 , are not desirable for use in bioceramics because of their carcinogenic nature. The using of these particles may lead to the toxicological effects in cells (Karunakaran et al. 2016).

The most promising reinforcers can be calcium HAp whiskers (Zhang et al. 2014; Yang et al. 2014) and carbon nanotubes (Mukherjee et al. 2014; Harrison et al. 2007).

HAp whiskers have such advantages as excellent biocompatibility, bioactivity and relatively poor chemical resistance. HAp whiskers are synthesized by the hydrothermal method at pressure up to 100 MPa, and the temperature varies from 80 to 400 °C (Zakaria et al. 2013; Yoshimura et al. 1997; Suchanek et al. 1994). The disadvantages of their usage are related to the fact that the high-temperature sintering of ceramic implants leads to the change in the form of particles. The elongated shape of particles disappears and as a result the strengthening effect decreases. Another promising way to increase the strength of the HA-based ceramics can be usage of multi-walled carbon nanotubes (MWCNTs) as reinforcers agents.

Carbon nanotubes have excellent mechanical properties, due to the strength of their carbon sp^2 bonds (White et al. 2007). MWCNTs also have structural similarity to the organic component of a bone. MWCNTs are similar in scale to type-I collagen fibrils in bone that is a few nanometers in diameter (Sadat-Shojai et al. 2013). The bioactivity and toxicity of carbon nanotubes (CNTs) in the composites for bone regeneration were discussed by White et al. (2007) and Roldo et al. (2013). As the additives, the MWCNTs in the composites may have no detrimental effects, and could even enhance its bioactive properties. It was indicated that MWCNTs can stimulate bone regeneration (Roldo et al.

2013), the formation of type-I collagen and are nontoxic in vivo (White et al. 2007). Recent studies also have shown that functionalized nanotubes may possess some bioactive properties (Tan et al. 2009; Park et al. 2014; Liu et al. 2018; Alshehri et al. 2016).

In this study, we synthesized and characterized ceramics for medical application with high biological activity and improved mechanical characteristics based on hydroxylapatite with additives of multi-walled carbon nanotubes. It was found that the increase of the amount of nanotubes leads to the increase of mechanical properties of ceramics.

Experiment

Materials

HAp ceramics were obtained from calcium phosphate powder that was synthesized as a result of a heterogeneous reaction between calcium carbonate (Merk, analytical grade) and orthophosphoric acid (Merk, analytical grade) (Zyman et al. 2000, 2008). The time of maturing was 24 h. The obtained calcium phosphate powder was centrifuged and dried in the air at a temperature of 90 °C. For the synthesis of HA, the resulting powder was calcinated at a temperature of 850 °C for 1 h in a wet atmosphere.

MWCNTs were prepared using the CVD method by decomposition of ethylene over the bimetallic Fe–Co/ Al_2O_3 catalyst at 670 °C (Usoltseva et al. 2007; Kuznetsov et al. 2012). This catalyst composition has been shown to provide MWCNTs of low defectiveness (Kuznetsov et al. 2014) and with low content of inorganic impurities. Scanning electron microscopy (SEM) analysis and energy-dispersive X-ray spectroscopy of MWCNTs were carried out on JEOL JSM-7500FA to evaluate surface morphology. The mean diameter of MWCNTs is 18 nm. According to EDX, the MWCNTs powder contains a small amount of catalyst less than 0.3 wt.%.

Synthesis of composite ceramics

Calcinated HAp powder was mechanically mixed with carbon nanotubes. The conditions (the total mass of HA and MWCNTs powders components during the mixing, rotation frequency and time of mixing) were the same for the all sets and samples in the sets. The concentration of MWCNTs in the composite material was 0.05, 0.1, 0.2 and 0.5 wt.%, respectively. Compacts were prepared from the powder in a disk form (3–5 mm height and 8 mm diameter) by uniaxial pressing under 120 MPa. All the compacts of HA with different concentration of the MWCNTs were sintered at 1100 °C for 1 h in the argon atmosphere. This atmosphere was used to prevent the oxidation effect of MWCNTs. In

White et al. (2010), it was shown that in the argon atmosphere there is the smallest loss of the nanotubes during the sintering of HA ceramics. In our experiment, the heating rate in the oven was 20 °C/min that was chosen by taking into account the results of the Mahajan et al. (2013). In the Mahajan et al. (2013), it was shown that at the heating rate above 20 K/min, the decomposition of MWCNTs is very small up to temperature 1200 °C.

Methods of study

Structural measurements were performed on a Philips APDW 40C diffractometer in copper K_α radiation ($\lambda = 0.154$ nm) with a nickel filter in the interval of diffraction angles 2θ from 20 to 70, with a scan step 0.01° and scan time for one step 1 s. The infrared spectroscopy (IR) has been carried out using a BIO-RAD FFS 175 spectrometer (Germany) with a resolution of 0.5 cm^{-1} in the frequency range between 400 and 4000 cm^{-1} . Scanning electron microscopy (SEM) analysis was carried out on JEOL JSM-7500FA at 20 kV to evaluate the surface morphology of the samples. The density of ceramic samples was measured by the Archimedes method for ten samples in each series. Microhardness tester Affri DM8 was used to measure the Vickers hardness. The compressive strength was measured employing an Instron-type testing machine.

Results and discussion

Diffraction patterns of ceramics with different concentration of MWCNTs are shown on Fig. 1. The XRD results of the derived samples were coherent with the Joint Committee on Powder Diffraction Standards (JCPDS-09-0432/1996). It is seen that all samples have apatite structure $P6_3/m$ (JCPDS-09-0432/1996). It resulted from the absence of any distinct reflections except those of HAp in the diffraction patterns. Any changes in the $P6_3/m$ structure are not observed for the different amount of nanotubes in the ceramics. The observed redistribution of the intensity of the reflections (112) and (300) is probably due to the texture. It indicates that in the argon atmosphere is possible of the significant loss of OH groups. In addition, sintering conditions (possible oxidation of nanotubes at a temperature of 1100 °C) contribute to the formation of carbonated hydroxyapatite.

The increasing of the width of the peaks with increasing the nanotube content is not observed. The average crystallite size $D \sim 50$ nm (coherent-scattering region) in the ceramics was estimated using the Scherrer's equation: $D = 0.9 \times \lambda / \beta \cos \theta$, where D is the crystallite size, $\lambda = 1.5418$ Å is the wavelength of CuK α , β is the full-width at half-maximum intensity (FWHM), and θ is Bragg's angle (Cullity 1978). It is seen from Fig. 1 that the broadening of the peaks is not

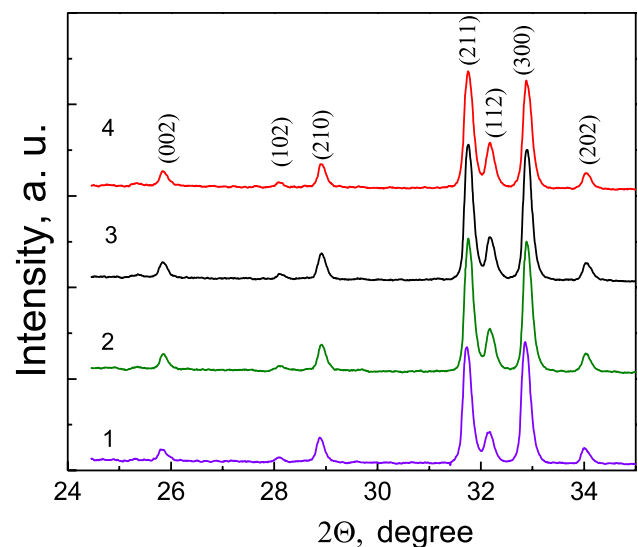


Fig. 1 XRD patterns of the ceramics synthesized at a temperature of 1100 °C in argon atmosphere: (1) hydroxyapatite (HAp) without additives of multi-walled carbon nanotubes (MWCNTs), (2) HAp with 0.05 wt.% MWCNTs, (3) HAp with 0.2 wt.% MWCNTs, and (4) HAp with 0.5 wt.% MWCNTs

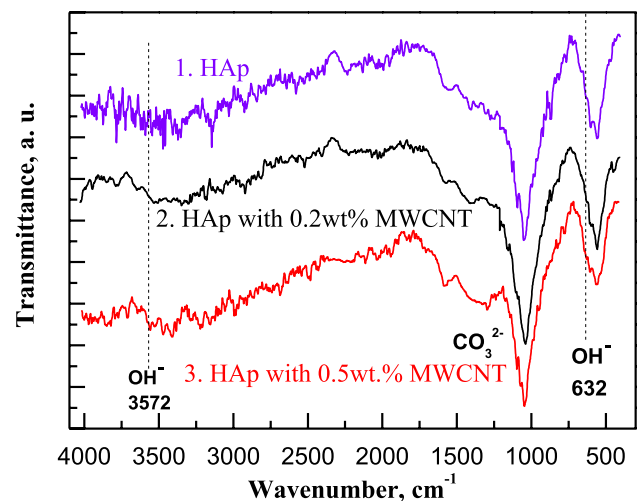


Fig. 2 FT-IR spectroscopy of ceramics synthesized at a temperature of 1100 °C in argon atmosphere: (1) hydroxyapatite (HAp) without additives of multi-walled carbon nanotubes (MWCNTs), (2) HAp with 0.2 wt.% MWCNTs, and (3) HAp with 0.5 wt.% MWCNTs

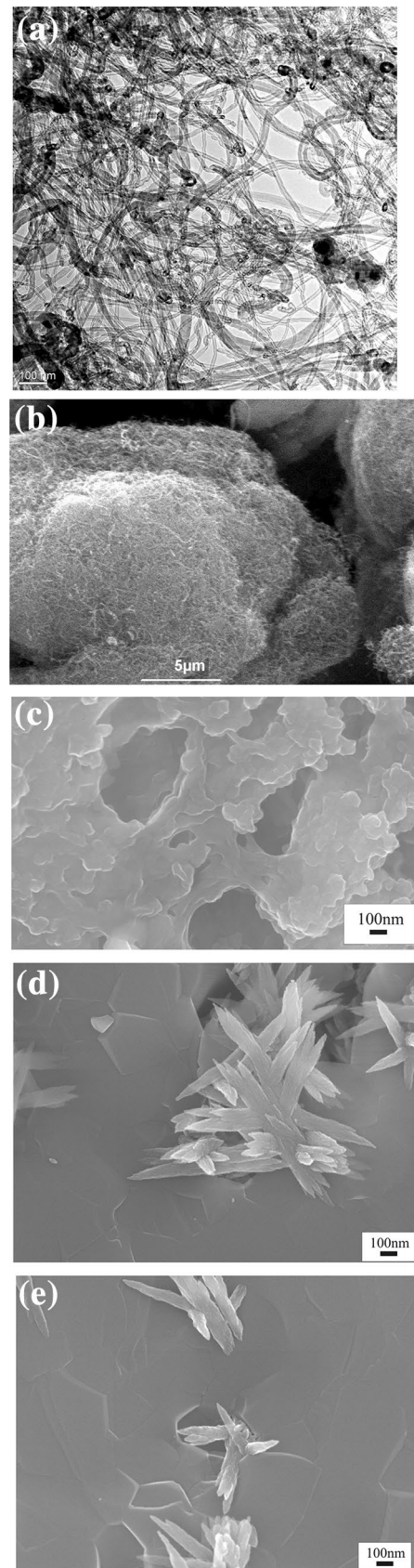
observed. It was found that in all samples, the change of D is less than several nanometers with the change of the MWCNTs concentration. Therefore, the impact on the microhardness of the change of the crystallite size is rather small.

The partial carbonization of ceramics is indicated by the results of IR studies shown in Fig. 2. It is seen that, apparently, carbonized apatite of A-type is predominantly formed. The stretching modes of OH^- (3572 cm^{-1}) are absent on the spectra. The intensity of vibration modes

Fig. 3 SEM images of the initial multi-walled carbon nanotubes (a), MWCNTs aggregates (b), pure HAp ceramic (c) and ceramic with 0.2 wt.% MWCNTs (d, e)

of OH^- (632 cm^{-1}) is weak that indicates that in our samples the A-type carbonized apatite was formed. Bands of PO_4^{3-} -vibrations in the ranges of $970\text{--}1100$ and $565\text{--}615\text{ cm}^{-1}$ are weakly separated. Broadband of stretching vibrations ($1400\text{--}1500\text{ cm}^{-1}$) characterizing of carbonate ions is present. With an increase of the amount of nanotubes in composite ceramics, the intensity of the carbonate stretching band increases, this may be due to partial oxidation of the nanotubes and as a result leads to more intensive carbonization of the apatite phase.

Electron microscopic studies of the initial multi-walled carbon nanotubes (Fig. 3a, b), pure ceramic (Fig. 3c) and ceramic with 0.2 wt.% nanotubes (Fig. 3d, e) are shown. The most part of the initial nanotubes have distributions of outer diameter $10\text{--}25\text{ nm}$ and the mean diameter of MWCNTs is 18 nm . The metal catalyst particles in MWCNTs are encapsulated inside the nanotubes between graphene layers (Fig. 3a) and would thus not influence the toxicity (White et al. 2007). The length and diameter of nanotubes also play role in cytotoxicity. Due to this, in the studies of the medical application of carbon nanotubes, the shift of interest from single-walled carbon nanotubes (SWNTs) that have small diameter ($1\text{--}2\text{ nm}$) to MWCNTs with higher diameter ($5\text{--}60\text{ nm}$) is observed. As reported, the thinner CNTs are more toxic than thicker ones (Rondo et al. 2013). As seen on Fig. 3b MWCNTs in the initial powder have the form of large aggregates that cannot be phagocytosed (Alshehri 2016). It is seen in the electron microscope images that the morphology of MWCNTs agglomerates significantly changed in the ceramics, but MWCNTs remains needle-like with an aspect ratio (length/diameter) of ~ 10 (Fig. 3d, e). It is also seen in Fig. 3c–e, that after mechanically mixed of HA powder with carbon nanotubes and further annealing at 1100 C the obtained ceramics have smaller porosity than the HA ceramic without MWCNTs additives. The obtained composite ceramics have two-phase structure: one phase is a hydroxyapatite matrix providing the necessary bioactivity of the material, and the other is agglomerates of carbon nanotubes located in the intergranular space of the matrix. MWCNTs take the role of collagen fibers and are able to decrease the stress intensity at the microcrack region, thus preventing further crack growth. According to the mechanical response modeling, the carbon nanotubes store most of the strain energy, since they are the stiffer phase in the composite (PourAkbar Saffar 2015). The sample of ceramic without nanotubes has a sufficient porosity (Fig. 3c). The nanotubes are placed along the grain boundaries of the apatite matrix and in the pores. The average grain size of the calcium–phosphate matrix does not exceed 300 nm , which



may indicate a high biological activity of the synthesized material.

The density of pure HAp ceramic is only 2.3 g/cm^3 (Fig. 4). The relative density was calculated using 3.156 g/cm^3 as the theoretical density of stoichiometric HA. The relative density of the pure HAp ceramic is 72.8%, and ceramic of HAp with additives of (MWCNTs) is 81.6% (samples with 0.2 wt.% MWCNTs) and 92.5% (samples with 0.5 wt.% MWCNTs). The presence of MWCNTs additives even in a small amount leads to obtaining a composite ceramics with higher density. This result is associated with partial oxidation of nanotubes and as a result with the appearing of carbon dioxide molecules in the local places of the sample during the sintering process (Merry et al. 1998). These molecules activate the sintering (Merry et al. 1998). In this case, the maximum rate of shrinkage is observed at temperatures that are almost 200°C below the sintering temperature of HA without additives (Zyman et al. 2011).

Figure 5 shows the compression strength of the HAp samples with different concentration of MWCNTs. It is seen that the compression strength increases with the increase of the amount of nanotubes in composite ceramics. The black line shows the median of the data at different concentration of MWCNTs. The blue square shows the maximum deviations from the mean values. The red line shows the interpolation curve. The observed increase in the spread of compressive strength values may be due to the inhomogeneous distribution of nanotubes in ceramics.

The Vickers microhardness of the ceramics is shown in Fig. 6. Vickers microhardness increases with the increase of the amount of nanotubes in composite ceramics. Due to the inhomogeneous distribution of nanotubes in ceramics, the difference between data of Vickers microhardness is greater in the samples with MWCNTs additives than in the case of pure HAp ceramics. At the same time, with the

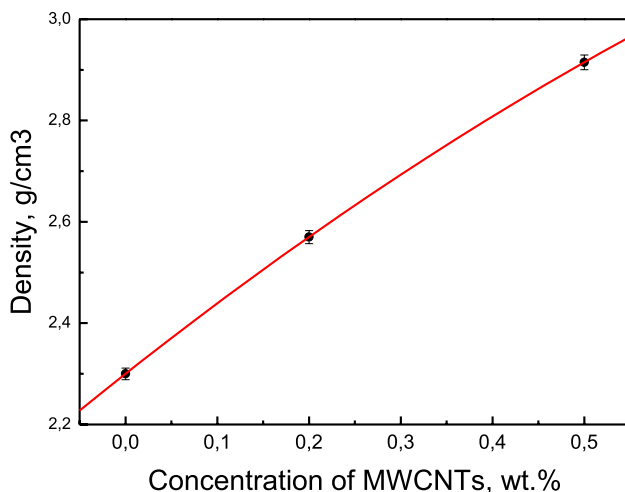


Fig. 4 Density of ceramics HAp vs. concentration of MWCNTs

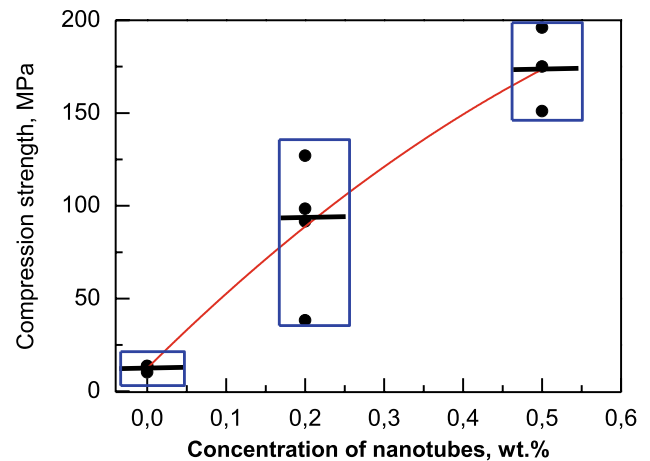


Fig. 5 Compression strength of the HAp samples with different concentration of MWCNTs

increase of the MWCNTs concentration, the scatter of data decreases, which indicates that with the increase of the amount of MWCNT their distribution in the samples are more homogeneous.

It should be noted that the porosity decreases (Fig. 4) and both compression strength (Fig. 5) and microhardness (Fig. 6) increase with the increase of the concentration of MWCNTs. Therefore, an increase of the mechanical characteristics of the composite can be associated both with the morphology of nanoparticles that play the role of centers of minimizing the propagation of cracks and with oxidation of MWCNTs, that leads to the formation of more dense carbonized ceramics.

To determine the main mechanism of one of these or their joint contribution in the increasing of mechanical characteristics of HAp, the additional research is required. The

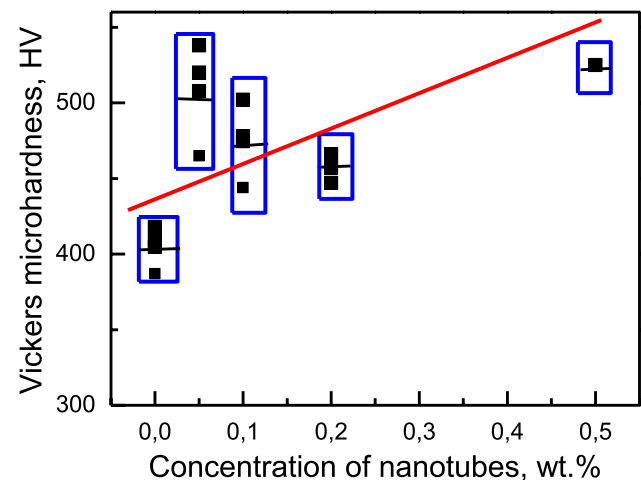


Fig. 6 Vickers microhardness of the HAp samples with different concentration of MWCNTs

hardness determines the ability of the crystalline to resist the plastic deformation during the penetration of an indenter, which results in the formation of new surfaces with the expenditure of the energy. For further analysis (separation of the hardness components: elastic deformation, plastic deformation, work on forming cracks and free surface) the additional investigations are required. The study of the relationship between the hardness and elastic modulus of this compound is one of the important next steps of the investigation. In the literature data, both a small increase and decrease of the Young's modulus (Y) of the ceramics are observed with the adding of MWCNTs. Lahiri observed ~ 30% increase of both the Vickers hardness and the Young's modulus for the sample of HA with 4 wt.% MWCNTs in comparison with pure HA. (Lahiri et al. 2010). This composite was obtained by Spark plasma sintering (SPS). The opposite effect was observed by Kealley (2008). It was found that for the composite "Synthesized HAp-5wt.% CNT" that obtained by the hot isostatic pressing (HIP) method, the Young's modulus is 7% smaller than for the initial pure synthesized HAp (Kealley 2008). Kalmodia discovered that adding about 1.6 wt.% CNT to the composite HA- Al_2O_3 decrease both Vickers hardness and Young's modulus by ~ 30% (Kalmodia et al. 2010). In her study as in the work of Lahiri, the composite was obtained using the method spark plasma sintering (SPS). Such contradictory results are likely to be due to the fact that different sintering conditions were chosen, as well as the fact that the tubes used in the experiments also have different values of the Young's modulus. In the article of Elumeeva et al., it is shown that the Young's modulus of MWCNTs depends on the diameter of the nanotubes and can vary from a $Y \sim 1000$ GPa (for tubes with diameter 7 nm) to $Y \sim 10$ GPa (diameter more than 40 nm) (Elumeeva et al. 2013). If the Young's modulus of the composite material is significantly different from the Young's modulus of human bone, mechanical stresses may occur, which can later lead to the destruction of the bone tissue near the implant. Considering the facts discussed above, we chose the MWCNTs with an average diameter of about 18 nm for sintering the composite. For nanotubes with mean diameters 18 nm, the Young modulus is $Y \sim 100$ GPa, which is comparable with the Young modulus of both pure HA (Lahiri 2010; Kealley 2008) and enamel in teeth (Oyen 2010). Thus, taken into account the fact that in our experiment Young's modulus of MWCNTs and HA are close, and also the fact that in our experiment the maximum concentration of nanotubes is almost ten times smaller than in Lahiri et al. (2010) and Kealley (2008), we do not expect a significant difference between the Young's modulus of the sintered composites and the initial HA ceramics.

The obtained composite materials with different contents of MCNT have hardness in the range of 4–5 GPa, which is comparable with the hardness of enamel. The hardness of

enamel has been reported in a range of 3.4–5.7 GPa and the elastic modulus in the range of 83.4–105.2 GPa (Oyen 2010). The compression strength of the obtained composites HA with MWCNTs is close to the values of the compression strength of the cortical bone 100–230 MPa (White et al. 2007). Thus, the investigation of the influence of small amounts of MWCNTs on the mechanical properties of the sintered HA composites has perspective for applications of using such new composites.

Conclusions

Ceramics for medical applications with high bioactivity and improved mechanical characteristics based on hydroxylapatite with a content of multi-walled carbon nanotubes have been synthesized and characterized. HAp has been prepared via the reaction of calcium carbonate and orthophosphoric acid. The mass ratio of reagents was chosen to obtain stoichiometric HAp. The phase composition and microstructure of synthesized bioceramics have been determined by XRD, IR and SEM. It was shown that in the process of sintering HAp-MWCNTs ceramics, partial oxidation of the nanotubes occurs, but the form of nanotubes remains needle-like. At the same time, the bioactive matrix consists of carbonated hydroxyapatite. With the increase of the concentration of nanotubes, the density and mechanical properties of the composites are significantly increased. The improvement of the mechanical characteristics of HAp-MWCNTs composite ceramics with increasing the nanotube concentration is apparently due to the fact that the presence of nanotubes in the intergranular space of the apatite matrix decreases the propagation of cracks. In this case, the higher stresses are required for the destruction of the material.

Acknowledgements The research is carried out within the framework of Tomsk Polytechnic University Competitiveness Enhancement Program and the Fundamental Research Program of the State Academies of Sciences for 2013–2020, line of research III.23.

References

- Ahn ES, Gleason NJ, Ying JY (2005) The effect of zirconia reinforcing agents on the microstructure and mechanical properties of hydroxyapatite-based nanocomposites. *J Am Ceram Soc* 88(12):3374–3379. <https://doi.org/10.1111/j.1551-2916.2005.00636.x>
- Ai M, Du Z, Zhu S, Geng H, Zhang X, Cai Q, Yang X (2017) Composite resin reinforced with silver nanoparticles—laden hydroxyapatite nanowires for dental application. *Dent Mater* 33(1):12–22. <https://doi.org/10.1016/j.dental.2016.09.038>
- Alshehri R, Ilyas AM, Hasan A, Arnaout A, Ahmed F, Memic A (2016) Carbon nanotubes in biomedical applications: factors, mechanisms, and remedies of toxicity. *J Med Chem* 59(18):8149–8167. <https://doi.org/10.1021/acs.jmedchem.5b01770>

- Buazar F, Alipouryan S, Kroushawi F, Hossieni SA (2014) Photodegradation of odorous 2-mercaptobenzoxazole through zinc oxide/hydroxyapatite nanocomposite. *Appl Nanosci* 5(6):719–729. <https://doi.org/10.1007/s13204-014-0368-4>
- Cullity BD (1978) Elements of X-ray diffraction, 2nd edn. Addison-Wesley, Boston, p 569
- Díaz M, Barba F, Miranda M, Guitián F, Torrecillas R, Moya JS (2009) Synthesis and antimicrobial activity of a silver–hydroxyapatite nanocomposite. *J Nanomater* 2009: 6 pages. <https://doi.org/10.1155/2009/498505>
- Elumeeva KV, Kuznetsov VL, Ischenko AV, Smajda R, Spina M, Forró L, Magrez A (2013) Reinforcement of CVD grown multi-walled carbon nanotubes by high temperature annealing. *AIP Adv* 3(11):112101. <https://doi.org/10.1063/1.4829272>
- Faingold A, Cohen SR, Shahar R, Weiner S, Rapoport L, Wagner HD (2014) The effect of hydration on mechanical anisotropy, topography and fibril organization of the osteonal lamellae. *J Biomech* 47:367–372. <https://doi.org/10.1016/j.jbiomech.2013.11.022>
- Goudarzi M, Batmanghelich F, Afshar A, Dolati A, Mortazavi (2014) Development of electrophoretically deposited hydroxyapatite coatings on anodized nanotubular TiO₂ structures: corrosion and sintering temperature. *Appl Surf Sci* 301:250–257. <https://doi.org/10.1016/j.apsusc.2014.02.055>
- Harrison BS, Atala A (2007) Carbon nanotube applications for tissue engineering. *Biomaterials* 28(2):344–353. <https://doi.org/10.1016/j.biomaterials.2006.07.044>
- Jadalannagari S, Deshmukh K, Ramanan S, Kowshik M (2013) Antimicrobial activity of hemocompatible silver doped hydroxyapatite nanoparticles synthesized by modified sol–gel technique. *Appl Nanosci* 4(2):133–141. <https://doi.org/10.1007/s13204-013-0197-x>
- Kalmodia S, Goenka S, Laha T, Lahiri D, Basu B, Balani K (2010) Microstructure, mechanical properties, and in vitro biocompatibility of spark plasma sintered hydroxyapatite–aluminum oxide–carbon nanotube composite. *Mater Sci Eng C* 30(8):1162–1169. <https://doi.org/10.1016/j.msec.2010.06.009>
- Karunakaran G, Rajendran V, Suriyaprabha R, Kannan N (2016) Influence of ZrO₂, SiO₂, Al₂O₃ and TiO₂ nanoparticles on maize seed germination under different growth conditions. *IET Nanobiotechnol* 10(4):171–177. <https://doi.org/10.1049/iet-nbt.2015.0007>
- Kealley CS, Latella BA, van Riessen A, Elcombe MM, Ben-Nissan B (2008) Micro- and nano-indentation of a hydroxyapatite–carbon nanotube composite. *J Nanosci Nanotech* 8(8):3936–3941. <https://doi.org/10.1166/jnn.2008.188>
- Kumar PH, Singh VK, Kumar P (2015) Mechanochemically synthesized kalsilite based bioactive glass–ceramic composite for dental veneering. *Appl Nanosci* 7(6):269–274. <https://doi.org/10.1007/s13204-015-0491-x>
- Kuznetsov VL, Krasnikov DV, Schmakov AN, Elumeeva KV (2012) In situ and ex situ resolved study of multi-component Fe–Co oxide catalyst activation during MWNT synthesis. *Phys Stat Solidi (B)* 249(12):2390–2394. <https://doi.org/10.1002/pssb.201200120>
- Kuznetsov VL, Bokova-Sirosh SN, Moseenkov SI, Ishchenko AV, Krasnikov DV, Kazakova MA, Obratsova ED (2014) Raman spectra for characterization of defective CVD multi-walled carbon nanotubes. *Phys Stat Solidi (B)* 251(12):2444–2450. <https://doi.org/10.1002/pssb.201451195>
- Kwok CT, Wong PK, Cheng FT, Man HC (2009) Characterization and corrosion behavior of hydroxyapatite coatings on Ti6Al4V fabricated by electrophoretic deposition. *Appl Surf Sci* 255(13):6736–6744. <https://doi.org/10.1016/j.apsusc.2009.02.086>
- Lahiri D, Singh V, Keshri AK, Seal S, Agarwal A (2010) Carbon nanotube toughened hydroxyapatite by spark plasma sintering: microstructural evolution and multiscale tribological properties. *Carbon* 48(11):3103–3120. <https://doi.org/10.1016/j.carbon.2010.04.047>
- Liu S, Li H, Zhang L, Hu D, Liu Q (2018) Preparation and characterization of implanted Fe catalyst in hydroxyapatite layer for uniformly dispersion carbon nanotube growth. *Appl Surf Sci* 455:75–83. <https://doi.org/10.1016/j.apsusc.2018.05.188>
- Mahajan A, Kingon A, Kukovec Á, Konya Z, Vilarinho PM (2013) Studies on the thermal decomposition of multiwall carbon nanotubes under different atmospheres. *Mater Lett* 90:165–168. <https://doi.org/10.1016/j.matlet.2012.08.120>
- Mansour SF, El-dek SI, Ahmed MA, Abd-Elwahab SM, Ahmed MK (2015) Effect of preparation conditions on the nanostructure of hydroxyapatite and brushite phases. *Appl Nanosci* 6(7):991–1000. <https://doi.org/10.1007/s13204-015-0509-4>
- Merry JC, Gibson IR, Best SM, Bonfield W (1998) Synthesis and characterization of carbonate hydroxyapatite. *J Mater Sci Mater Med* 9(12):779–783. <https://doi.org/10.1023/a:1008975507498>
- Mocanu A, Furtos G, Rapuntean S, Horovitz O, Flore C, Garbo C, Tomoaia-Cotisel M (2014) Synthesis; characterization and antimicrobial effects of composites based on multi-substituted hydroxyapatite and silver nanoparticles. *Appl Surf Sci* 298:225–235. <https://doi.org/10.1016/j.apsusc.2014.01.166>
- Mukherjee S, Kundu B, Sen S, Chanda A (2014) Improved properties of hydroxyapatite–carbon nanotube biocomposite: mechanical, in vitro bioactivity and biological studies. *Ceram Intern* 40(4):5635–5643. <https://doi.org/10.1016/j.ceramint.2013.10.158>
- Ol'khovik LP, Tkachenko MV, Kamzin AS (2011) Physicotechnological principles of the development of biocompatible magnetic nanoparticles for medicine. *Bull Russ Acad Sci Phys* 75(2):281–283. <https://doi.org/10.3103/s1062873810031025>
- Oyen ML (2010) Handbook of nanoindentation: with biological applications. Pan Stanford Publishing, Redwood City
- Padovani GC, Feitosa VP, Sauro S, Tay FR, Durán G, Paula AJ, Durán N (2015) Advances in dental materials through nanotechnology: facts, perspectives and toxicological aspects. *Trends Biotechnol* 33(11):621–636. <https://doi.org/10.1016/j.tibtech.2015.09.005>
- Park JE, Park IS, Neupane MP, Bae TS, Lee MH (2014) Effects of a carbon nanotube–collagen coating on a titanium surface on osteoblast growth. *Appl Surf Sci* 292:828–836. <https://doi.org/10.1016/j.apsusc.2013.12.058>
- Phan BTN, Nguyen HT, Đào HQ, Pham LV, Quan TTT, Nguyen DB, Vu TT (2016) Synthesis and characterization of nano-hydroxyapatite in maltodextrin matrix. *Appl Nanosci* 7(1–2):1–7. <https://doi.org/10.1007/s13204-016-0541-z>
- Pour Akbar Saffar K, Sudak LJ, Federico S (2015) A biomechanical evaluation of CNT-grown bone. *J Biomed Mater Res Part A* 104(A):465–475. <https://doi.org/10.1002/jbm.a.35582>
- Puvvada N, Panigrahi PK, Kalita H, Chakraborty KR, Pathak A (2012) Effect of temperature on morphology of triethanolamine-assisted synthesized hydroxyapatite nanoparticles. *Appl Nanosci* 3(3):203–209. <https://doi.org/10.1007/s13204-012-0133-5>
- Radha G, Balakumar S, Venkatesan B, Vellaichamy E (2015) Evaluation of hemocompatibility and in vitro immersion in microwave-assisted hydroxyapatite–alumina nanocomposites. *Mater Sci Eng C* 50:143–150. <https://doi.org/10.1016/j.msec.2015.01.054>
- Roldo M, Fatouros DG (2013) Biomedical applications of carbon nanotubes. *Annu Rep Sect C (Phys Chem)* 109:10–35. <https://doi.org/10.1039/c3pc90010j>
- Sadat-Shojai M, Khorasani MT, Dinpanah-Khoshdargi E, Jamshidi A (2013) Synthesis methods for nanosized hydroxyapatite with diverse structures. *Acta Biomater* 9(8):7591–7621. <https://doi.org/10.1016/j.actbio.2013.04.012>
- Shrivastava S, Dash D (2009) Applying nanotechnology to human health: revolution in biomedical sciences. *J Nanotechnol* 184702:14. <https://doi.org/10.1155/2009/184702>
- Suchanek W, Yashima M, Kakihana M, Yoshimura M (1997) Hydroxyapatite/hydroxyapatite–whisker composites without sintering additives: mechanical properties and microstructural

- evolution. *J Am Ceram Soc* 80(11):2805–2813. <https://doi.org/10.1111/j.1151-2916.1997.tb03197.x>
- Sung YM, Shin YK, Ryu JJ (2007) Preparation of hydroxyapatite/zirconia bioceramic nanocomposites for orthopedic and dental prosthesis applications. *Nanotechnology* 18(6):065602. <https://doi.org/10.1088/0957-4484/18/6/065602>
- Supraja N, Prasad TNVKV, David E (2015) Synthesis, characterization and antimicrobial activity of the micro/nano structured biogenic silver doped calcium phosphate. *Appl Nanosci* 6(1):31–41. <https://doi.org/10.1007/s13204-015-0409-7>
- Tan Q, Zhang K, Gu S, Ren J (2009) Mineralization of surfactant functionalized multi-walled carbon nanotubes (MWNTs) to prepare hydroxyapatite/MWNTs nanohybrid. *Appl Surf Sci* 255(15):7036–7039. <https://doi.org/10.1016/j.apsusc.2009.03.036>
- Usoltseva A, Kuznetsov V, Rudina N, Moroz E, Haluska M, Roth S (2007) Influence of catalysts' activation on their activity and selectivity in carbon nanotubes synthesis. *Phys Stat Solidi (B)* 244(11):3920–3924. <https://doi.org/10.1002/pssb.200776143>
- White AA, Best SM, Kinloch IA (2007) Hydroxyapatite–carbon nanotube composites for biomedical applications. A review. *Int J Appl Ceram Technol* 4(1):1–13. <https://doi.org/10.1111/j.1744-7402.2007.02113.x>
- White AA, Kinloch IA, Windle AH, Best SM (2010) Optimization of the sintering atmosphere for high-density hydroxyapatite–carbon nanotube composites. *J R Soc Interface* 7(5):529–539. <https://doi.org/10.1098/rsif.2010.0117.focus>
- Xu J, Yang Y, Wan R, Shen Y, Zhang (2014) Hydrothermal preparation and characterization of ultralong strontium-substituted hydroxyapatite whiskers using acetamide as homogeneous precipitation reagent. *Sci World J*. <https://doi.org/10.1155/2014/863137>
- Yoshimura M, Suda H, Okamoto K, Ioku K (1994) Hydrothermal synthesis of biocompatible whiskers. *J Mater Sci* 29(13):3399–3402. <https://doi.org/10.1007/bf00352039>
- Yu J, Zhang W, Li Y, Wang G, Yang L, Jin J, Huang M (2014) Synthesis, characterization, antimicrobial activity and mechanism of a novel hydroxyapatite whisker/nano zinc oxide biomaterial. *Biomed Mater* 10(1):015001. <https://doi.org/10.1088/1748-6041/10/1/015001>
- Zakaria SM, Sharif Zein SH, Othman MR, Yang F, Jansen JA (2013) Nanophase hydroxyapatite as a biomaterial in advanced hard tissue engineering: a review. *Tissue Eng Part B Rev* 19(5):431–441. <https://doi.org/10.1089/ten.teb.2012.0624>
- Zhang MY, Cheng GJ (2010) Nanoscale size dependence on pulsed laser sintering of hydroxyapatite/titanium particles on metal implants. *J Appl Phys* 108(11):113112. <https://doi.org/10.1063/1.3504612>
- Zyman Z, Tkachenko M (2011) CO₂ gas-activated sintering of carbonated hydroxyapatites. *J Eur Ceram Soc* 31(3):241–248. <https://doi.org/10.1016/j.jeurceramsoc.2010.09.005>
- Zyman Z, Ivanov I, Rochmistrov D, Glushko V, Tkachenko N, Kijko S (2000) Sintering peculiarities for hydroxyapatite with different degrees of crystallinity. *J Biomed Mater Res* 54(2): 256–263. [https://doi.org/10.1002/1097-4636\(200102\)54:2%3C256::aid-jbm13%3E3.0.co;2-b](https://doi.org/10.1002/1097-4636(200102)54:2%3C256::aid-jbm13%3E3.0.co;2-b)
- Zyman ZZ, Tkachenko MV, Polevodin DV (2008) Preparation and characterization of biphasic calcium phosphate ceramics of desired composition. *J Mater Sci Mater Med* 19(8):2819–2825. <https://doi.org/10.1007/s10856-008-3402-9>

Publisher's Note Springer Nature remains neutral with regard to jurisdictional claims in published maps and institutional affiliations.